AL-Bahir
Journal for Engineering and Pure Sciences
BJEPS

Volume 1 | Issue 1 Article 3

In silico Evaluation of the Antimalarial Potential of the Phytoconstituents of the Azadirachta indica Plant

Areh E.T.
Department of Chemistry, Confluence University of Science and Technology, P.M.B. 1040, Osara, Kogi State, Nigeria

Atolani O.
Department of Chemistry, University of Ilorin, P.M.B. 1515, Ilorin, Nigeria

Kambizi L
Department of Horticulture, Cape Peninsula University of Technology, South Africa

Recommended Citation

E.T., Areh; O., Atolani; and L, Kambizi (2022) "In silico Evaluation of the Antimalarial Potential of the Phytoconstituents of the Azadirachta indica Plant," *Al-Bahir*: Vol. 1: Iss. 1, Article 3.
Available at: https://doi.org/10.55810/2313-0083.1004

ORIGINAL STUDY

In silico Evaluation of the Antimalarial Potential of the Phytoconstituents of the *Azadirachta indica* Plant

Ekundayo T. Areh [a,*], Olubunmi Atolani [b], Learnmore Kambizi [c]

[a] Department of Chemistry, Confluence University of Science and Technology, P.M.B. 1040, Osara, Kogi State, Nigeria
[b] Department of Chemistry, University of Ilorin, P.M.B. 1515, Ilorin, Nigeria
[c] Department of Horticulture, Cape Peninsula University of Technology, South Africa

Abstract

Background and objectives: **Malaria, a parasitic protozoan disease caused primarily by *Plasmodium falciparum*, has killed millions of people in Africa, particularly those with meager or no access to orthodox medical facilities and therapies. Extracts from the *Azadirachta indica* (neem) plant is believed to possess antimalaria properties among the locals that rely on herbs. Numerous in - vivo studies have suggested the antimalarial properties of neem extract and phytochemicals. This study employs an *in - silico* method through molecular docking techniques to provide insight while adding credence to the antimalarial potential of phytochemicals of neem plants as claimed in folkloric medicine.**

Methods: **− The crystal structure of *P. falciparum a causative parasite of malaria* was retrieved from the Protein Data Bank, and *Azadirachta indica* phytochemicals were obtained from the PubChem database. Molecular docking through virtual screening was carried out on the characterized phytochemicals. The bioactive compounds from the *Azadirachta indica* plant were investigated by docking with the crystal structure of *P. falciparum* receptor and compared with standard antimalarial drugs (lumenfrantrine and artemisinin).**

Results: **Three *Azadirachta indica* phytochemicals (gedunnin, nimbinene and salanin) shows a competing binding energy and affinity when compared to the approved antimalarial drugs (lumefrantrine and artemisinin). While the binding affinities for azadirachtin, nimbandiol and quercetin is lower than the affinity in artemisinin but comparable with lumefrantrine.**

Conclusion: **This virtual screening verified and identified a potential phytochemical component of antimalarial properties against a protein target: 1m7o, *P. falciparum* triosephosphate isomerase (PfTIM).**

Keywords: *In silico*, *Azadiracta indica*, *Plasmodium falciparum*, Phytochemical, 3-Phosphoglycerate (3 PG)

1. Introduction

Malaria is a major global public health problem. Six *Plasmodium* species can infect human with *Plasmodium falciparum* being the most frequent, virulent and lethal species among the malarial parasites which accounts for ninety one percent (91%) of malaria cases worldwide of which the majority (about 86%) occurs in the Africa region (more prevalent in Sub-Saharan Africa) [1−4]. *P. falciparum* is the agent of severe malaria and responsible for most malarial deaths [2,5−7].

Malaria is a devastating transferrable and infectious disease that is transmitted through female anopheles mosquito infected with *Plasmodium species* [6,8]. The vector, female anopheles mosquito introduces the parasite that causes malaria into the human blood through its saliva when feeding or during a blood meal [8−11]. When the parasite get into the human body in the form of sporozoites it moves from the blood stream to the hepatocytes in the liver where it mature, reproduce and multiply asexually over the next 7−12 days, during this time there are no symptoms [6,8,12]. The parasites now in the form of merozoites, leaves the liver cells (in vesicle) to the bloodstream after traveling through the heart to the capillaries of the lungs [8,12]. The vesicles eventually disintegrate and release the

Received 3 July 2022; revised 18 July 2022; accepted 6 August 2022.
Available online 2 September 2022

* Corresponding author.
E-mail address: arehekundayotimi@gmail.com (E.T. Areh).

https://doi.org/10.55810/2313-0083.1004

merozoites to enter the bloodstream where it invades and multiply in the erythrocytes [8]. Clinical symptoms of malaria resulting for the invasion and rapture of erythrocytes cell by merozoites include fever, chills, headache, vomiting, muscle ache, respiratory distress, cough, anorexia, rigor, diarrhea, severe anemia, abdominal discomfort, thrombocytopenia, seizures, hypoglycemia, metabolic acidosis, hyperlactemia, coma associated with increased intracranial pressure (cerebral malaria), and complications of pregnancy, which include preterm birth and low birth weight due to fetal growth restriction [6,8,13,14].

In some infected blood cells, instead of replicating asexually, the merozoites develop into sexual forms (gametocytes), which circulate in the bloodstream and are ingested during mosquito bites. The ingested gametocytes develop in the mosquito into mature sex cell (gametes) which later develop into ookinetes that actively burrow through the mid-gut of the mosquito and form oocysts, which further develop into thousands of active sporozoites. The oocyst eventually bursts, releasing sporozoites that travel to the salivary glands of the mosquito, the cycle of human infection begins again when the mosquito bites another person [4,8].

P. species infection vary in severity depending on the species and host factors, the host factor include the level of host immunity, which is linked to the past infection of *Plasmodium* parasite [6,15,16]. *Plamodium ovale* and *Plasmodium vivax* have dormant forms (called hypnozoites) which can emerge from the liver years after the initial infection, which can lead to relapse if not treated properly [6,17]. In *P. falciparum*, but not other *P. species* that affect human malarias, the transition to gametocytogenesis is delayed and the peak of gametocytaemia is 7–10 days after that of asexual parasitaemia, blood-stage infection can persist for months or years in *P. falciparum* infections when untreated [10]. In tropical regions, *P. vivax* relapses typically every 3–4 weeks. In temperate areas, *P. vivax* can remain latent for 8–10 months between primary infection and first relapse [18] . Recurrent *P. falciparum* and *vivax* malaria have pronounced adverse effects in young children and interfere with growth, development and schooling [10].

The development of drug in *P. falciparum* (most especially drug resistance) strains has stimulated considerable interest in the search for new antimalarial drugs and drug targets [7]. Natural products offers a wide range for drug discovery to cure diseases and drug resistance disease [19–21]. Phytochemical from *Azadirachta indica* has been documented to possess many pharmacological activities against numerous diseases most especially it anti-malarial properties [22]. This present study is to assess the *in-silico* antimalarial properties of the phytochemicals from *Azadirachta Indica*.

Azadirachta indica (Neem), of the family Meliaceae, commonly called dogonyaro in some parts of Nigeria, is an evergreen plant native to India, where it is known as divine tree or life-giving tree. It is commonly found in America but is more endemic to tropical and subtropical regions. It is a tall tree with a height ranging between 20 and 40 m with scaly and hard bark, alternating branches and leaves, small white flowers, and green drupes fruits that turn yellowish when ripening. Its flowering and fruiting seasons range between the months of May–June and June–August respectively [23,24]. The taxonomical classification is as indicated in Table 1.

Compounds that exhibited bioactivities such as antioxidant, antiviral, antimicrobial, anti-inflammatory, antiulcer and antifungal activities have been isolated from leaves, bark, roots, fruit and seeds of *Azadirachta indica*. Its pharmacological activities are due to the presence of alkaloids, flavonoids, saponins, terpenes, tannins, and phenols [23,25,26]. The most reported and bioactive constituents in *Azadirachta indica* (Table 2) are azadirachtin, gedunin, nimbandiol, nimbin, nimbinene, nimbolide, nimbolinin, nimbidin, salannin and quercetin [24,26–28].

2. Materials and method

2.1. Computational platform and software

All computation analyses were performed on an Acer ES1-131-C271, Windows 10 Home Single Language 64-bit operating system, Intel Celeron N3150 @ 1.6 GHz 8.00 GB RAM. Software used for the screening are; OpenbabeL, PyRx, AutoDock4, AutoDock Vina, PyMOL, LigPlot + Version 2.2.5 and Discovery Studio.

Table 1. Botanical taxonomic of neem plant.

Taxonomy	Classification
Order	Rutales
Suborder	Retinae
Family	Meliaceae
Subfamily	Melioideae
Tribe	Melieae
Genus	Azadirachta
Species	indica
Latin	*Azadirachta indica*
Indian	Holy tree
Hindi	Neem, Nim
Hausa	Dogonyaro
Igbo	Ogwu Akuma

Table 2. Phytochemical constituents of Azadirachta indica *and reported biological activities.*

Phytochemical	Class of compound	Activities	Reference
Azadirachtin	tetranortriterpenoid	Anticancer, antimalarial	[27,29,30]
Gedunin	Limonoid tetranortriterpenoid	Anticancer, antimalarial	[22,27,31]
Nimbandiol	pentanortriterpenoids		[27]
Nimbine	Triterpenoid	Anti-inflammatory, antipyretic, antiseptic	[27]
Nimbinene	pentanortriterpenoids		[27]
Nimbolide	tetranortriterpenoids	Anticancer, antimalarial, antibacterial	[27,32]
Salannin	pentanortriterpenoids		[27]
Quercetin	Polyphenolic flavonoid		[27]
Nimbidin		Anti-inflammatory, anti-fungal, antibacterial	[33]

Openbabel was used to convert file to PDB file format, PyRx was used to minimized the energy and prepare the ligand, AutoDock4 was used in protein preparation and to obtain the grid parameter of the protein, AutoDock Vina was used to execute the virtual screening in CMD, PyMOL was used to export ligand and protein into ligand-protein complex, LigPlot+ was used to obtain the two dimension (2-D) ligand-protein interactions, Discovery Studio was used to view the three dimension (3-D) ligand–protein interactions.

2.2. Retrieval of ligand and preparation

Azadirachta indica phytochemicals with potent antimalarial properties and available at the NCBI Pub Chem Compounds data bank (https://pubchem.ncbi.nlm.nih.gov/) were considered for this study.

The two-dimensional (2D) structures of the selected phytochemicals, approved drugs and the co-crystallized ligand were obtained in the simple data file (sdf) from the NCBI Pub Chem Compounds data bank (https://pubchem.ncbi.nlm.nih.gov/) and were converted into pdb file format using Openbabel in PyRx [34]. The ligands (3-Phosphoglycerate, phytochemicals and approved drugs) were further prepared for molecular docking by minimizing the energy in PyRx using mmff94 energy minimization parameter following the method described in Dallakyan and Olson 2015 with slight modification [35]. The ligand details are indicated in Table 3.

2.3. Retrieval of protein, active site prediction and preparation

The crystal structure of *P. falciparum* triosephosphate isomerase (PfTIM) provides an insights into antimalarial drug discovery and design [36], this crystal structure complied with substrate analog 3-phosphoglycerate (3 PG), PDB Code: 1M7O (Fig. 1) available at RCSB Protein Data Bank possess a basic structural representation for others PfTIM crystals. The three-dimensional (3-D) X-ray crystal structure of the protein *P. falciparum* triosephosphate isomerase (PfTIM) with the native 3-phosphoglycerate (3 PG), PDB Code: 1M7O obtained through X-ray diffraction with a resolution of 2.40 Å used in this study was retrieved from the RCSB Protein Data Bank.

The crystal structure of *P. falciparum* triosephosphate isomerase (PfTIM) has two active sites (chain A and Chain B). Therefore, for detailed docking and better analysis the chains were separated. The receptor chains were split and prepared for molecular docking in AutoDock4 by the removal the water molecules, the co-crystallized ligand and other heteroatoms (Fig. 2). The missing residue was repaired, histidine hydrogen was added, polar hydrogen was added, converted to AD4 type and the grid dimension around the active site (residues bounded to the native ligands) was obtained using AutoDock4 following the protocol described in Ravi and Krishnan 2016 with slight modification [37]. The grid dimension around the active site was obtained in AutoDock4 and site values for the crystal structure of *P. falciparum* triosephosphate isomerase (PfTIM) subunit A and B used in this docking are given in Table 4.

2.4. In silico *molecular docking and validation of docking*

The docking setting for this virtual screening was validated by re-docking the native ligand into crystal structure of *P. falciparum* triosephosphate isomerase (PfTIM-Chain A and Chain B separately) and interactions were compared with un-dock crystal structure of *P. falciparum* triosephosphate isomerase in subunit A and B chains.

The virtual screening was processed to estimate the binding affinities and interaction of the ligands (phytochemicals, approved drugs and 3-Phosphoglycerate) against prepared crystal structure of *P.*

Table 3. Drugs and phytochemical details.

Drug/Compound	Pubchem CID	Molecular formula	Molecular weight	Structure
3-Phosphoglycerate	724	$C_3H_7O_7P$	186 g/mol	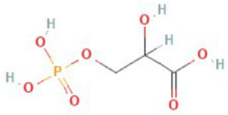
Lumefantrine Approved drug	6437380	$C_{30}H_{32}NOCl_3$	528 g/mol	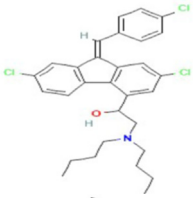
Artemisinin Approved drug	68827	$C_{15}H_{22}O_5$	282 g/mol	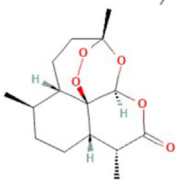
Azadirachtin	5281303	$C_{35}H_{44}O_{16}$	720 g/mol	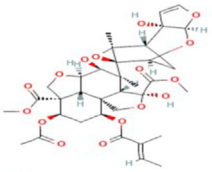
Gedunin	12004512	$C_{28}H_{34}O_7$.	482 g/mol	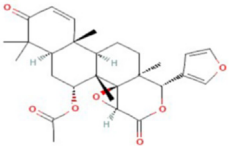
Nimbandiol	157277	$C_{26}H_{32}O_7$	456 g/mol	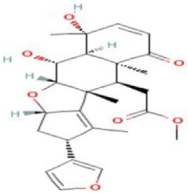
Nimbinene	44715635	$C_{28}H_{34}O_7$	482 g/mol	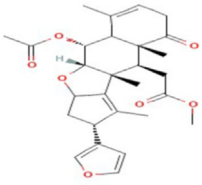
Quercetin	5280343.	$C_{15}H_{10}O_7$	302 g/mol	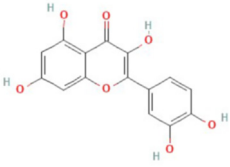

(*continued on next page*)

Table 3. (continued)

Drug/Compound	Pubchem CID	Molecular formula	Molecular weight	Structure
Salanin	6437066	$C_{34}H_{44}O_9$.	596 g/mol	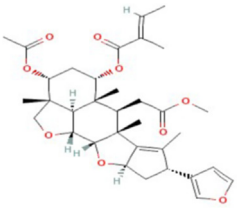

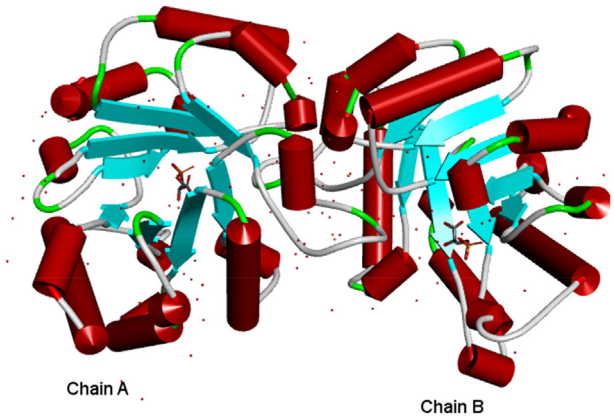

Fig. 1. Crystal structure of Plasmodium falciparum *triosephosphate isomerase (PfTIM) with native ligand 3-Phosphoglycerate (Discovery Studio-schematic display style).*

falciparum triosephosphate isomerase (PfTIM). Trott and Olson 2009 methods were adopted in the virtual screening with slight modification [38]. For high accuracy and reliability, this *in silico* study uses an exhaustiveness of ten in the molecular docking procedure.

Table 4. Docking grid for the crystal structure of PfTIM.

Chain	Spacing	Dimensions (Npts)	Center
A	0.375	X - 50	X - 8.361
		Y - 52	Y - 13.389
		Z - 38	Z - 23.556
B	0.375	X - 40	X - 19.528
		Y - 40	Y - -14.139
		Z - 50	Z - 22.056

3. Results

3.1. Docking setting validation

Validation was performed by re-docking the native ligand into the crystal structure of *P. falciparum* triosephosphate isomerase (PfTIM-chain A and Chain B) and superpose with the original-undock crystal structure of *P. falciparum* triosephosphate isomerase. The interaction, pose and superpose were visualized in LigPlot + for its validity (Fig. 3a and 3b).

The superpose image obtained in Fig. 3a*(iii)* and Fig. 3b*(iii)* shows a comparative and reliable validation for the docking procedure adopted for this

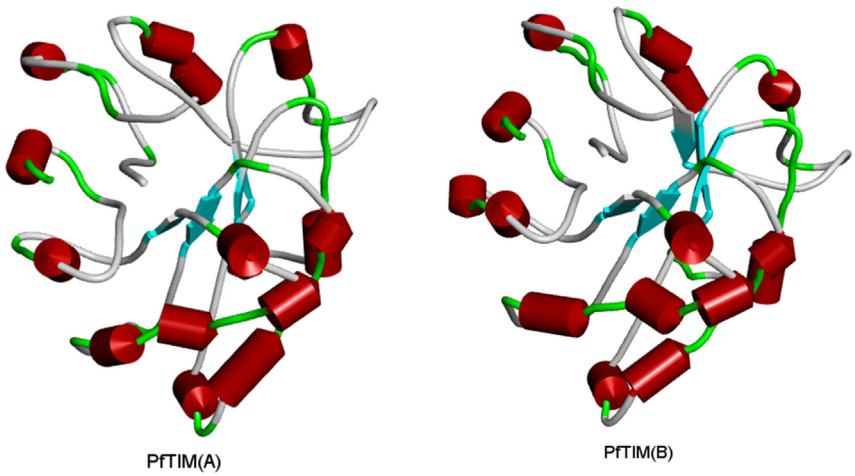

Fig. 2. Crystal structure of Plasmodium falciparum *triosephosphate isomerase (PfTIM) chain A and chain B (Discovery Studio-schematic display style).*

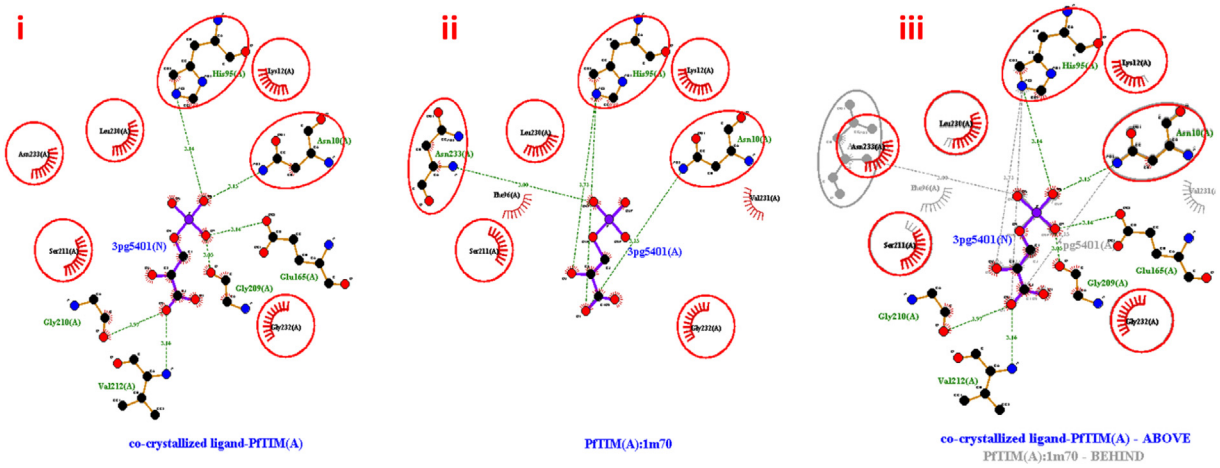

Fig. 3a. Crystal structure of Plasmodium falciparum *triosephosphate isomerase (PfTIM) A subunit with (i) redock native ligand (ii) native ligand (iii) superimposed complexes (redock native ligand-PfTIM complex and native ligand-PfTIM complex).*

virtual screening. For complexes (redocked and undock) obtained in PfTIM A subunit, the protein residues; ASN10, LYS12, HIS95, SER211, LEU230, GLY232 and ASN233 superpose well (Fig. 3a). Also, the protein residues; ASN10, LYS12, HIS95, GLY209, LEU230, VAL231 and GLY232 generated in PfTIM B subunit complexes superimpose properly (Fig. 3b) with few exceptions.

3.2. Docking (virtual screening)

From the docking-screening process using AutoDock Vina command prompt with the vina_windows.pl script, only the best or top ranked docked complexes were extracted from the result generated from the virtual screening. The main interaction, bonds category and types between the ligand and the protein were obtained in the non-bond section in Discovery Studio (Table 5).

The ligand conformation with the best docking value was combined with the prepared PfTIM in PyMOL, the 2-dimension (2-D) and 3-dimension (3-D) visual interactions were obtained in LigPlot+ and Discovery Studio respectively. All visual interactions for all screening ligands are shown in *Supplementary figures* (Fig. 5) at the Appendix section.

3.3. Bond interaction and affinity comparison

Bond interactions (electrostatic, hydrogen and hydrophobic) enhance the binding affinity and biological activity of complex molecules and help in stabilizing the biochemical environment of target–drug complexes, also ligand-protein interaction with more hydrogen bond tend to form a stronger complex with high binding affinity [39–41].

From the binding energy value (Table 5), the binding affinities of the crystal structure of PfTIM

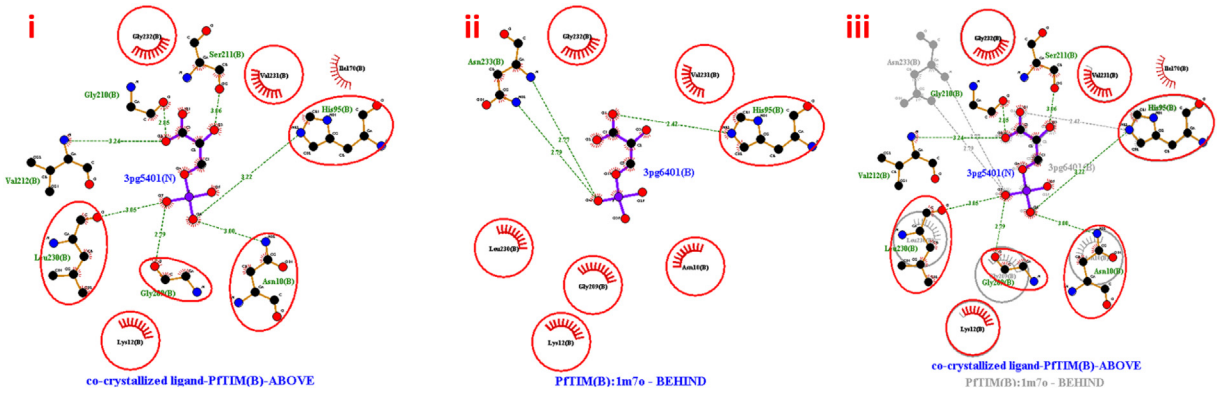

Fig. 3b. Crystal structure of Plasmodium falciparum *triosephosphate isomerase (PfTIM) B subunit with (i) redock native ligand (ii) native ligand (iii) superimposed complexes (redock native ligand-PfTIM complex and native ligand-PfTIM complex).*

Table 5. The interactions of ligands with PfTIM from the docking evaluation.

COMPOUND	PfTIM CHAIN A				PfTIM CHAIN B			
	Energy/affinity (kcal/mol)	Interaction	Bond Category	Type	Energy/affinity (kcal/mol)	Interaction	Bond Category	Type
3-phospho Glycerate (3 PG)	−4.9	LYS12:NZ - 3 PG:O	Hydrogen	Conventional	−4.9	ASN10:HD21 - 3 PG:O	Hydrogen	Conventional
		HIS95:HE2 - 3 PG:O	Hydrogen	Conventional		HIS95:HE2 - 3 PG:O	Hydrogen	Conventional
		GLY232:HN - 3 PG:O	Hydrogen	Conventional		3 PG:P - LEU230:O	Hydrogen	Conventional
		3 PG:H - LEU230:O	Hydrogen	Conventional		3 PG:H - GLU165:OE2	Hydrogen	Conventional
		3 PG:H - LEU230:O	Hydrogen	Conventional				
		3 PG:H - SER211:OG	Hydrogen	Conventional				
		3 PG:H - GLY210:O	Hydrogen	Conventional				
Lumefantrine (LUM)	−6.5	GLU238:OE2 - LUM	Electrostatic	Pi-Anion	−6.4	LUM:C - ASN65:OD1	Hydrogen	Carbon Hydrogen
		SER19:CB - LUM	Hydrophobic	Pi-Sigma		ARG98:NH1 - LUM	Electrostatic	Pi-Cation
		LUM:C - LEU236	Hydrophobic	Alkyl		PHE102 - LUM	Hydrophobic	Pi—Pi Stacked
		LUM:C - LYS237	Hydrophobic	Alkyl		LUM:C - VAL78	Hydrophobic	Alkyl
		LUM:Cl - ILE20	Hydrophobic	Alkyl		LUM:Cl - VAL44	Hydrophobic	Alkyl
		LUM:Cl - LEU23	Hydrophobic	Alkyl		LUM:Cl - ARG98	Hydrophobic	Alkyl
		LUM:Cl - LEU236	Hydrophobic	Alkyl		HIS95 - LUM:Cl	Hydrophobic	Pi-Alkyl
		TRP11 - LUM:Cl	Hydrophobic	Pi-Alkyl		LUM - CYS13	Hydrophobic	Pi-Alkyl
		LUM - LEU23	Hydrophobic	Pi-Alkyl		LUM - VAL44	Hydrophobic	Pi-Alkyl
		LUM - LEU236	Hydrophobic	Pi-Alkyl		LUM - CYS13	Hydrophobic	Pi-Alkyl
		LUM - LEU23	Hydrophobic	Pi-Alkyl		LUM - ARG98	Hydrophobic	Pi-Alkyl
Artemisinin (ART)	−7.3	LYS12:NZ - ART:O	Hydrogen	Conventional	−6.8	ART:C - ILE63	Hydrophobic	Alkyl
		GLY232:HN - ART:O	Hydrogen	Conventional		ART:C - VAL78	Hydrophobic	Alkyl
		ALA234 - ART:C	Hydrophobic	Alkyl				
		ART - ILE170	Hydrophobic	Alkyl				
		ART:C - ILE170	Hydrophobic	Alkyl				
		HIS95 - ART:C	Hydrophobic	Pi-Alkyl				
		PHE96 - ART:C	Hydrophobic	Pi-Alkyl				
Azadirachtin (AZA)	−6.9	PHE96:HO - AZA:O	Hydrogen	Conventional	−7.1	ARG99:HH11 - AZA:O	Hydrogen	Conventional
		ARG99:HH11 - AZA:O	Hydrogen	Conventional		ASP106:HN - AZA:O	Hydrogen	Conventional
		GLN133:HE21 - AZA:O	Hydrogen	Conventional		GLN133:NE2 - AZA:O	Hydrogen	Conventional
		GLN146:NE2 - AZA:O	Hydrogen	Conventional				
		AZA:H - ASP106:OD2	Hydrogen	Conventional		GLN146:NE2 - AZA:O	Hydrogen	Conventional
						AZA:C - GLY128:O	Hydrogen	Carbon Hydrogen
		ARG99:CD - AZA:O	Hydrogen	Carbon Hydrogen		AZA:C - ILE170:O	Hydrogen	Carbon Hydrogen
		VAL142 - AZA	Hydrophobic	Alkyl		LEU167 - AZA	Hydrophobic	Alkyl
		LYS145 - AZA	Hydrophobic	Alkyl				
		AZA - VAL142	Hydrophobic	Alkyl				
		AZA - LYS145	Hydrophobic	Alkyl				
		AZA:C - LYS100	Hydrophobic	Alkyl				
		AZA:C - LEU167	Hydrophobic	Alkyl				

Gedunin (GED)	−8.0	GED:C - PHE102	Hydrophobic	Pi-Sigma	−7.8	ARG99:HH11 - GED:O	Hydrogen	Conventional
		GED:C - VAL44	Hydrophobic	Alkyl		ASP106:HN - GED:O	Hydrogen	Conventional
		GED:C — CYS13	Hydrophobic	Alkyl		ARG99:CD - GED:O	Hydrogen	Carbon Hydrogen
		GED - ILE63	Hydrophobic	Pi-Alkyl				
		GED - VAL78	Hydrophobic	Pi-Alkyl				
Nimbandiol (NIML)	−7.2	LYS237:NZ - N:NIML	Electrostatic	Pi-Cation	−7.6	NIML:H - GLY209:O	Hydrogen	Conventional
		ALA234 - NIML	Hydrophobic	Alkyl		LYS237:NZ - NIML	Hydrogen; Electrostatic	Pi-Cation; Pi-Donor Hydrogen
						ALA234 - NIML	Hydrophobic	Alkyl
						NIML:C - ILE170	Hydrophobic	Alkyl
Nimbinene (NIME)	−8.4	ARG98:NH1 - NIME:O	Electrostatic	Attractive Charge	−7.8	ARG98:NH1 - NIME:O	Hydrogen	Conventional
		ARG98:NH1 - NIME:O	Hydrogen	Conventional		ARG98:HD1 - NIME:O	Hydrogen	Carbon Hydrogen
		ARG98:HD1 - NIME:O	Hydrogen	Carbon Hydrogen		NIME:C — CYS13	Hydrophobic	Alkyl
		NIME:C - GLN64:O	Hydrogen	Carbon Hydrogen		HIS95 - NIME:C	Hydrophobic	Pi-Alkyl
		NIME:C — CYS13	Hydrophobic	Alkyl		PHE102 - NIME:C	Hydrophobic	Pi-Alkyl
		PHE102 - NIME:C	Hydrophobic	Pi-Alkyl		NIME - VAL78	Hydrophobic	Pi-Alkyl
		NIME - VAL78	Hydrophobic	Pi-Alkyl				
Quercetin (QUE)	−7.2	QUE:H - ASN65:O	Hydrogen	Conventional	−7.1	QUE:H - ASN65:O	Hydrogen	Conventional
		QUE:H — HIS95:ND1	Hydrogen	Conventional		ARG98:NH1 - QUE	Hydrogen; Electrostatic	Pi-Cation; Pi-Donor Hydrogen
		QUE:H - GLU97:OE1	Hydrogen	Conventional		ARG98:NH1 - QUE	Electrostatic	Pi-Cation
		ARG98:NH1 — QUE	Hydrogen; Electrostatic	Pi-Cation; Pi-Donor Hydrogen		QUE - ARG98	Hydrophobic	Pi-Alkyl
		ARG98:NH1 — QUE	Electrostatic	Pi-Cation				
		QUE - ARG98	Hydrophobic	Pi-Alkyl				
Salannin (SAL)	−7.7	LYS145:HZ1 - SAL:O	Hydrogen	Conventional	−7.1	GLN133:NE2 - SAL:O	Hydrogen	Conventional
		LEU167:CD1 - SAL	Hydrophobic	Pi-Sigma		LYS145:CE - SAL:O	Hydrogen	Carbon Hydrogen
		ARG99 - SAL	Hydrophobic	Alkyl				
		SAL:C - ARG99	Hydrophobic	Alkyl		LYS100:NZ - SAL	Electrostatic	Pi-Cation
		SAL:C - LEU167	Hydrophobic	Alkyl		LEU167:CD1 - SAL	Hydrophobic	Pi-Sigma
		SAL:C - VAL142	Hydrophobic	Alkyl		ARG99 - SAL	Hydrophobic	Alkyl
		SAL:C - LYS145	Hydrophobic	Alkyl		LYS100 - SAL	Hydrophobic	Alkyl
		SAL - LYS100	Hydrophobic	Pi-Alkyl		SAL:C - ARG99	Hydrophobic	Alkyl
						SAL:C - LEU167	Hydrophobic	Alkyl
						SAL:C - VAL142	Hydrophobic	Alkyl
						SAL:C - LYS145	Hydrophobic	Alkyl
						SAL - LYS100	Hydrophobic	Pi-Alkyl

Table 6. Nimbandiol- PfTIM bonds and energy comparison.

Complex	Nimbandiol- PfTIM subunit A			Nimbandiol- PfTIM subunit		
Energy	−7.2 kcal/mol			−7.6 kcal/mol		
Bonds	Electrostatic	Hydrogen	hydrophobic	Electrostatic	Hydrogen	hydrophobic
Number	1	–	1	1	2	2

Table 7. Gedunin nimbinene, salanin and artemisnin bond affinities with PfTIM subunit A.

Compound	Artemisnin	Gedunin	Nimbinene	Salanin
Binding energy (kcal/mol)	−7.3	−8.0	−8.4	−7.7
Electrostatic (attractive charge) bond	–	–	1	–
Electrostatic (Pi-cation)	–	–	–	–
Hydrogen (Conventional) bond	2	–	1	1
Hydrogen (Carbon) bond	–	–	2	–
Hydrophobic (Alkyl) bond	3	2	1	5
Hydrophobic (Pi-Alkyl) bond	2	2	2	1
Hydrophobic (Pi-Sigma) bond	–	1	–	–
Total interactions	7	5	7	7

subunits with a particular ligand is dependent on the number of bonds or interactions; gedunin-PfTIM A subunit (−8.0 kcal/mol) five interactions and gedunin-PfTIM B subunit (−7.8 kcal/mol) three interactions, nimbandiol-PfTIM A subunit (−7.2 kcal/mol) two interactions and nimbandiol-PfTIM B subunit (−7.6 kcal/mol) four main interactions, nimbinene-PfTIM A subunit (−8.4 kcal/mol) seven interactions and nimbinene-PfTIM B subunit (−7.8 kcal/mol) six interactions, quercetin-PfTIM A subunit (−7.2 kcal/mol) six interactions and quercetin-PfTIM B subunit (−7.1 kcal/mol) four main interaction. However, this trend was not seen in salanin and azadirachtin, difference in binding energy may be due to other factor apart from the number of interactions.

Ligand-protein interaction that show a binding affinity which depends on the nature of bonds between the ligand and the subunits crystal structure of PfTIM is nimbandiol, with binding value of −7.2 kcal/mol in PfTIM subunit A and −7.6 kcal/mol PfTIM subunit B (Table 6).

Finally, nimbinene has the highest docking value with binding affinities of −8.4 kcal/mol in PfTIM subunit A, this may be due to present of electrostatic bond through attractive charge, as it is the only phytochemical and ligand that possess this type of electrostatic bond in this study.

3.4. Ligand comparison and promising phytochemical

The amino residue interactions in some ligand-protein complexes of this study were also found in the research work of Parthasarathy et al., (2002) in which it was reported that the active-site of the

Table 8. Gedunin nimbinene, salanin and artemisnin bond affinities with PfTIM subunit B.

Compound	Artemisinin	Gedunin	Nimbinene	Salanin
Binding energy (kcal/mol)	−6.8	−7.8	−7.8	−7.1
Electrostatic (attractive charge) bond	–	–	–	–
Electrostatic (Pi-cation)	–	–	–	1
Hydrogen (Conventional) bond	–	2	1	1
Hydrogen (Carbon) bond	–	1	1	1
Hydrophobic (Alkyl) bond	2	–	1	6
Hydrophobic (Pi-Alkyl) bond	–	–	3	1
Hydrophobic (Pi-Sigma) bond	–	–	–	–
Total interaction	2	3	6	10

crystal structure of PfTIM are LYS12, HIS95, GLU165 and that the interaction of ligand atom 3-phosphoglycerate (3 PG) occurs at amino residues ASN10, LYS12, HIS95, GLU165, and LEU230 protein residue of PfTIM [42]. The protein residue interaction (of *Azadirachta indica* Phytochemical-crystal structure of PfTIM) in this study which are also found in the work of Parthasarathy et al., (2002) are; HIS95 subunit B – Lumefantrine:Cl, LYS12:NZ subunit A - Artemisinin:O, HIS95 subunit A - Artemisinin:C, HIS95 subunit B - Nimbinene:C and Quercetin:H – HIS95:ND1 subunit A . The amino residue HIS95 is predominant, which is a residue on the active site of the crystal structure of PfTIM subunit A and B.

The binding affinities of the approved antimalarial drug (Table 5), shows that artemisinin has a better binding affinity than its counterpart lumefantrine in subunit A and B of the crystal structure of PfTIM, which supports and confirms that artemisinin-based combination therapy is more effective in the treatment of malaria than lumefantrine-based combination therapy [43]. In subunit A PfTIM the binding affinity of lumefantrine is −6.5 kcal/mol while artemisinin is −7.3 kcal/mol, this may be due to the interaction of artemisinin with some of the protein residue at the active site of the crystal structure of PfTIM; LYS12:NZ - Artemisinin:O and HIS95 - Artemisinin:C.

All the screen phytochemical shows a high binding affinity than lumefantrine which may indicate that all the phytochemical can be a good substitute to this drug. Azadirachtin, nimbandiol and quercetin show a comparative binding energy with artemisinin at subunit A and B crystal structure of PfTIM. Gedunin, nimbinene and salanin show a relative high binding affinity than artemisinin which will be consider for further discussion based the nature of the bond category and type (Table 7 and Table 8).

The electrostatic (attractive charge) bond and hydrophobic (Pi-sigma) bonds present in nimbinene-PfTIM subunit A and gedunin-PfTIM subunit A respectively may be responsible for its high binding affinities (Table 7).

In the ligand-protein interactions in crystal structure of PfTIM subunit B, less number of interactions and the absence of strong force of interactions (electrostatic and hydrogen bond) may be responsible for the low binding affinity in artemisinin (Table 8).

4. Conclusion

In conclusion, most of the investigated phytochemicals from *Azadirachta indica* exhibited comparative antimalarial activities against 1m7o: Plasmodium falciparum trisephosphate isomerase (PfTIM). The findings in this work further add credence to the claim that *Azadirachta indica* extracts are potent against malaria infection. Further *in vivo* studies are recommended for the evaluation of each phytochemical and their synergistic antimalarial effects.

Likewise, there is also the need to further investigate other reported isolates of *Azadirachta indica* against other species of causative enzyme of malaria to underscore the mechanism of action, molecular dynamic and validate the potency of the phytochemicals as antimalarial agent(s).

Source of funding

This research did not receive any grants or funds from funding agencies in the commercial, public or not-for-profit sector.

Conflict of interest

The authors have no conflicts of interest.

Appendix

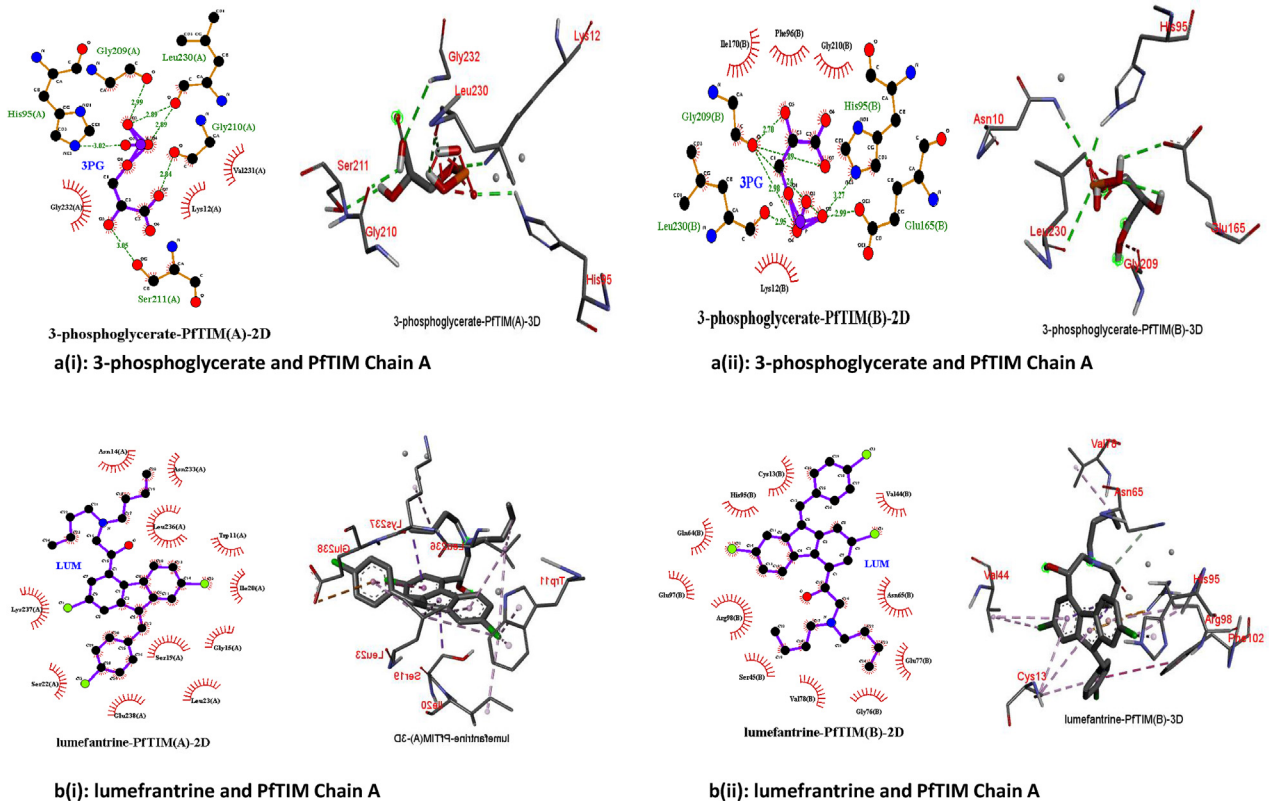

Supplementary Fig. 5. 2-dimension (2-D) and 3-dimension (3-D) visual interactions in LigPlot+ and Discovery Studio respectively.

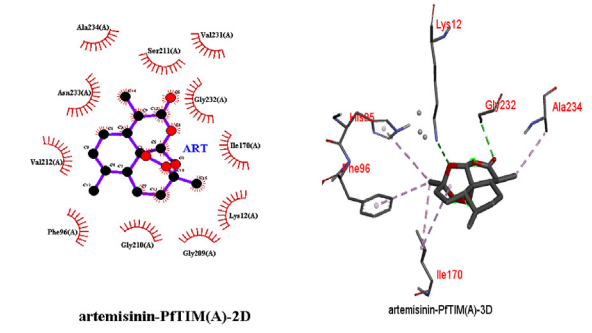

c(i): artemisinin and PfTIM Chain A

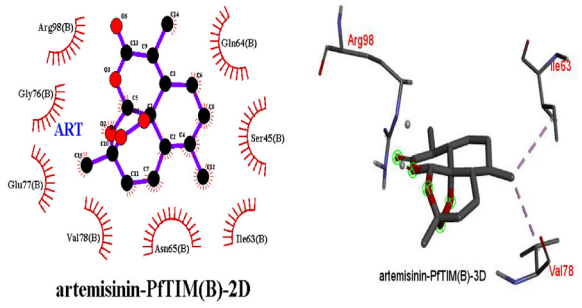

c(ii): artemisinin and PfTIM Chain B

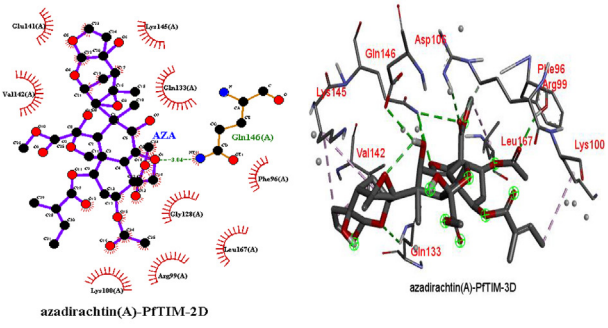

d(i): azadirachtin and PfTIM Chain A

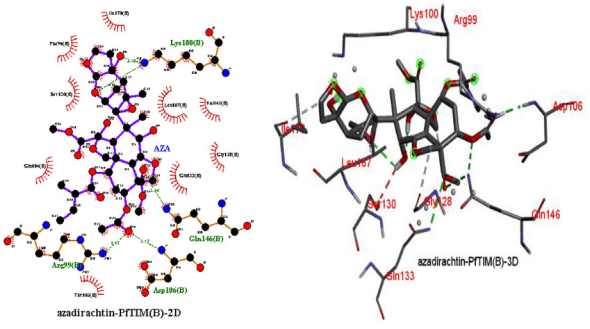

d(ii): azadirachtin and PfTIM Chain B

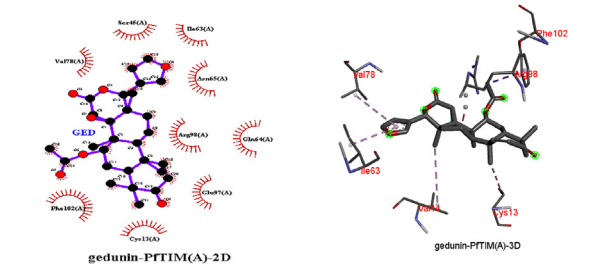

e(i): gedunin and PfTIM Chain A

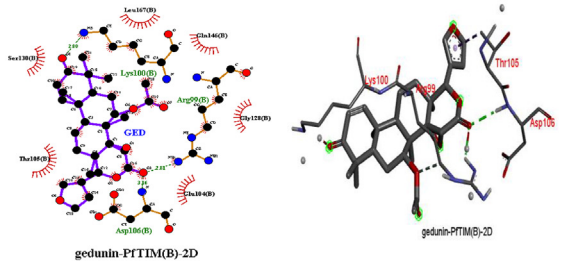

e(ii): gedunin and PfTIM Chain B

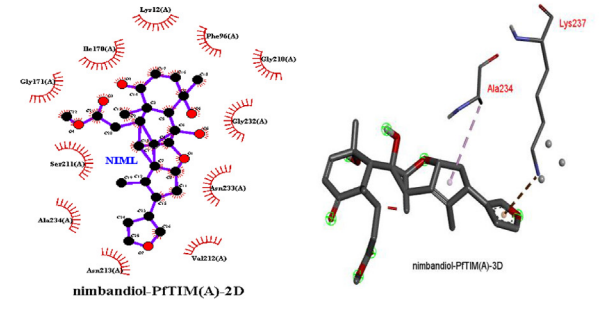

f(i): nimbandiol and PfTIM Chain A

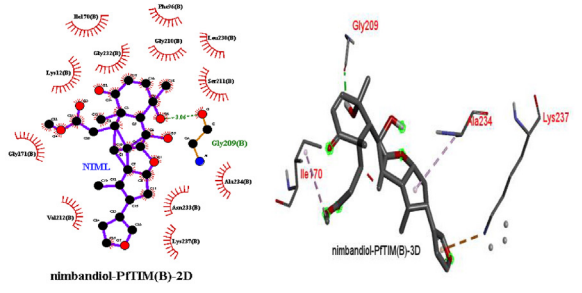

f(ii): nimbandiol and PfTIM Chain B

Supplementary Fig. 5. (Continued).

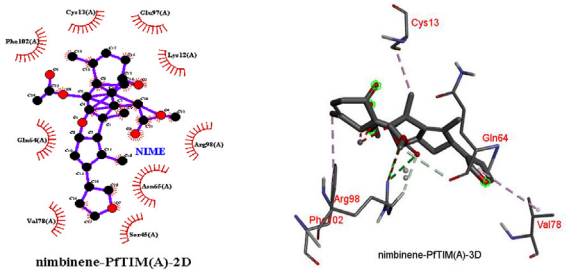

g(i): nimbinene and PfTIM Chain A

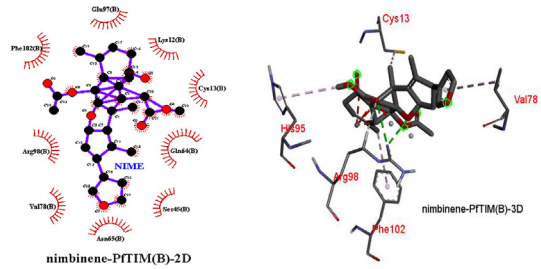

g(ii): nimbinene and PfTIM Chain B

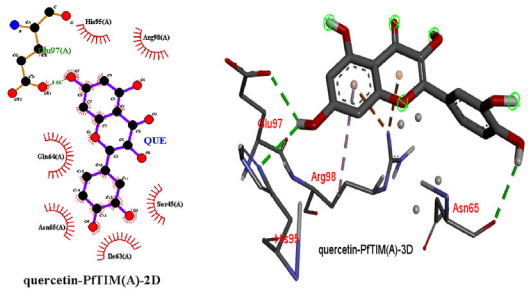

h(i): quercetin and PfTIM Chain A

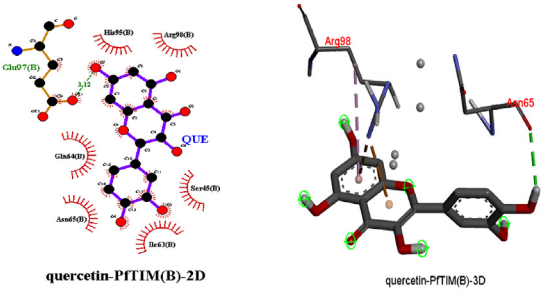

h(ii): quercetin and PfTIM Chain B

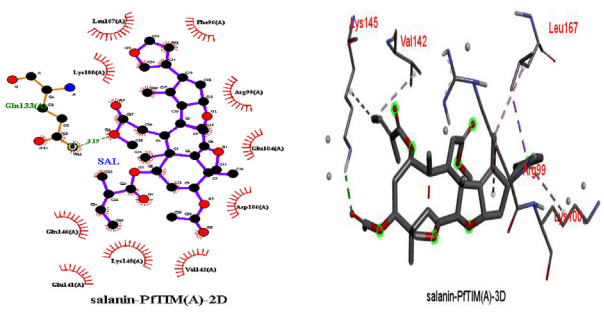

i(i): Salanin and PfTIM Chain A

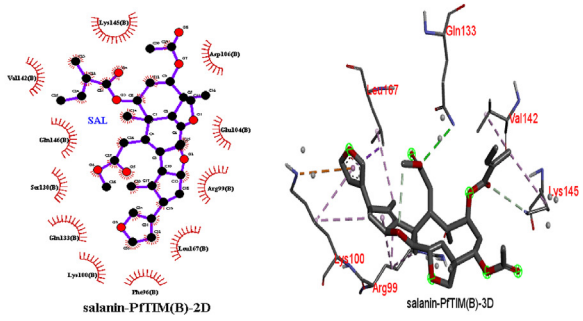

i(ii): Salanin and PfTIM Chain B

KEYS FOR 2D AND 3D INTERACTIONS

Ligplot+ 2D interactions

- Hydrogen bond (oxygen and hydrogen) only
- Non-ligand residues involved in hydrophobic contact(s) and Non hydrogen-oxygen bonds (carbon hydrogen bonds)
- Corresponding atoms involved in hydrophobic contact(s)

Discovery Studio (3D) interactions

- Conventional hydrogen bond
- Carbon hydrogen Bond
- Electrostatic (Attractive Charge) bond
- Hydrophobic (pi-pi sigma) bond
- Hydrophobic (pi-sigma) bond
- Hydrophobic (alkyl) bond

Supplementary Fig. 5. (Continued).

References

[1] Arévalo-Herrera M, Lopez-Perez M, Medina L, Moreno A, Gutierrez JB, Herrera S. Clinical profile of Plasmodium falciparum and Plasmodium vivax infections in low and unstable malaria transmission settings of Colombia. Malar J 2015;14(154):1–11.

[2] Joste V, Maurice L, Bertin GI, Aubouy A, Boumédiène F, Houzé S, et al.. Identification of Plasmodium falciparum and host factors associated with cerebral malaria: description of the protocol for a prospective, case-control study in Benin (NeuroCM). BMJ Open 2019;9(5):1–9.

[3] Ravindra G, Balaram P. Plasmodium falciparum triosephosphate isomerase : new insights into an old enzyme*. Pure Appl Chem 2005;77(1):281–9.

[4] Perkins DJ, Were T, Davenport GC, Kempaiah P, Hittner JB, Michael J. Severe malarial anemia: innate immunity and pathogenesis. Int J Biol Sci 2011;7(9):1427–42.

[5] Neves BJ, Braga RC, Melo-Filho CC, Moreira-Filho JT, Muratov EN, Andrade CH. QSAR-based virtual screening: advances and applications in drug discovery. Front Pharmacol 2018;9(1275):1–7.

[6] Phillips MA, Burrows JN, Manyando C, Huijsduijnen RH Van, Voorhis WC Van, Wells TNC. Malaria. Primer 2017; 3(17050):1–24.

[7] Parthasarathy S, Ravindra G, Balaram H, Balaram P, Murthy MRN. Structure of the Plasmodium falciparum triosephosphate isomerase - phosphoglycolate complex in two crystal forms: characterization of catalytic loop open and closed conformations in the ligand-bound state. Biochemistry 2002;41(44):13178–88.

[8] Mawson AR. The pathogenesis of malaria: a new perspective. Pathog Glob Health 2013;107(3):122–9.

[9] Miller LH, Ackerman HC, Su X, Wellems TE. Malaria biology and disease pathogenesis: insights for new treatments. Nat Med 2013;19(2):156–67.

[10] White NJ, Pukrittayakamee S, Hien TT, Faiz MA, Mokuolu OA, Dondorp A. Malaria. Lancet 2014;383:723–35.

[11] Cowman AF, Healer J, Marapana D, Marsh K. Malaria: biology and disease [Internet] Cell 2016;167(3):610–24. Available from: https://doi.org/10.1016/j.cell.2016.07.055.

[12] Haldar K, Murphy SC, Milner DA, Taylor TE. Malaria: mechanisms of erythrocytic infection and pathological correlates of severe disease. Annu Rev Pathol Mech 2007;2: 217–49.

[13] Schofield BL, Hackett F. Signal transduction in host cells by a glycosylphosphatidyllnositol toxin of malaria parasites by louis schofield and fiona hackett. Natl Institute Med Res 1993;177:145–58.

[14] Warren GL, Andrews CW, Capelli AM, Clarke B, LaLonde J, Lambert MH, et al.. A critical assessment of docking programs and scoring functions. J Med Chem 2006;49(20): 5912–31.

[15] Wassmer S, Grau G. Severe malaria: what's new on the pathogenesis front? Int J Parasitol 2016;47:1–8.

[16] Wassmer SC, Taylor TE, Rathod PK, Mishra SK, Mohanty S, Arevalo-herrera M, et al.. Investigating the pathogenesis of severe malaria: a multidisciplinary and cross-geographical approach. Am J Trop Med Hyg 2015;93(Suppl 3):42–56.

[17] White NJ. Determinants of relapse periodicity in Plasmodium vivax malaria. Malar J 2011;10(297):1–35.

[18] Simpson J, Aarons L, Collins W, Jeffery G, White N. Population dynamics of untreated Plasmodium falciparum malaria within the adult human host during the expansion phase of the infection. Parasitology 2002;124:247–63.

[19] Newman DJ, Cragg GM. Natural products as sources of new drugs over the nearly four decades from 01/1981 to 09/2019. J Nat Prod 2019 [A-AH].

[20] Thomford NE, Senthebane DA, Rowe A, Munro D, Seele P, Id AM, et al.. Natural products for drug discovery in the 21st century: innovations for novel drug discovery. Int J Mol Sci 2018;19(1578):1–29.

[21] Abdel-razek AS, El-naggar ME, Allam A, Morsy OM, Othman SI. Microbial natural products in drug discovery. Processes 2020;8(470):1–19.

[22] Khalid SA, Duddeck H, Gonzalez-Sierra M. Isolation and characterization of an antimalarial agent of the neem tree Azadirachta Indica. J Nat Prod 1989;52(5):922–7.

[23] Ujah II, Nsude CA, Ani ON, Alozieuwa UB, Okpako IO, Okwor AE. Phytochemicals of neem plant (Azadirachta indica) explains its use in traditional medicine and pest control. GSC Biol Pharm Sci 2021;14(2):165–71.

[24] Alzohairy MA. Therapeutics role of azadirachta indica (Neem) and their active constituents in diseases prevention and treatment. Evid base Compl Alternative Med 2016; 2016(7382506):1–11.

[25] Ukaoma A, Nwachukwu MO, Ukaoma VO, Adjeroh LO, Urenus I. Phytochemical and antimicrobial activity of neem seed oil (azadirachta indica) on bacteria isolates. J Chem Inf Model 2019;7(2):1–19.

[26] Ogbuewu IP, Odoemenam VU, Obikaonu HO, Opara MN, Emenalom OO, Uchegbu MC, et al.. The growing importance of neem (Azadirachta indica A. Juss) in agricultrue, industry, medicine and environment: a review. Res J Med Plant 2011;5:230–45.

[27] Sarah R, Tabassum B, Idrees N, Hussain MK. Bioactive compounds isolated from neem tree and their application (April 2020). Springer; 2019. p. 1–27.

[28] Srivastava SK, Agrawal B, Kumar A, Pandey A. Phytochemicals of AzadirachtaIndica source of active medicinal constituent used for cure of various diseases: a review. J Sci Res 2020;64(1):385–90.

[29] Bhowmik D, Yadav J, Tripathi KK, Kumar KPS, Pradesh U. Herbal remedies of Azadirachta indica and its medicinal application. J Chem Pharmaceut Res 2010;2(1):62–72.

[30] Achi NK, Onyeabo C, Nnate DA, Ekeleme-Egedigwe CA, Kalu IK, Chibundu IC, et al.. Therapeutic effects of Azadirachta indica A.Juss. leaves in malaria-induced male Wistar rats. J Pharm Pharmacogn Res 2018;6(3):191–204.

[31] Braga TM, Rocha L, Chung TY, Oliveira RF, Oliveira AI, Morgado J, et al.. Biological activities of gedunin — a limonoid from the Meliaceae family. Molecules 2020;25(493):1–24.

[32] Subramani R, Gonzalez E, Arumugam A, Ortega A, Bonkoungou S, Narayan M, et al.. Nimbolide inhibits pancreatic cancer growth and metastasis through ROS-mediated apoptosis and inhibition of epithelial-to- mesenchymal transition. Sci Rep 2016;6(19819):1–12.

[33] Biswas K, Chattopadhyay I, Banerjee RK. Biological activities and medicinal properties of neem (Azadirachta indica). Curr Sci 2002;82(11):1336–45.

[34] Boyle NMO, Banck M, James CA, Morley C, Vandermeersch T, Hutchison GR. Open Babel : an open chemical toolbox. J Chem Inf Model 2011;3(33):1–14.

[35] Dallakyan S, Olson AJ. Small-molecule library screening by docking with PyRx. Methods Mol Biol 2015;1263:243–50.

[36] Velanker SS, Ray SS, Gokhale RS, Suma S, Balaram H, Balaram P, et al.. Triosephosphate isomerase from Plasmodium falciparum : the crystal structure provides insights into antimalarial drug design. Structure 1997;5(6):751–61.

[37] Ravi L, Krishnan K. A handbook on protein-ligand docking tool: autodock4. Innovare J Med Sci 2016;4(3):1–6.

[38] Trott O, Olson AJ. Software news and update AutoDock vina: improving the speed and accuracy of docking with a new scoring function, efficient optimization, and multithreading. J Comput Chem 2009;31(2):455–61.

[39] Patil R, Das S, Stanley A, Yadav L, Sudhakar A. Optimized hydrophobic interactions and hydrogen bonding at the target-ligand interface leads the pathways of drug-designing. PLoS One 2010;5(8):1–10.

[40] Salentin S, Schreiber S, Haupt VJ, Adasme MF, Schroeder M. PLIP: fully automated protein – ligand interaction profiler. Nucleic Acids Res 2015;43(April:443–7.

[41] Stojanovi S, Zari SD. Hydrogen bonds and hydrophobic interactions of porphyrins in porphyrin-containing proteins. Open Struct Biol J 2009;3:34–41.

[42] Parthasarathy S, Balaram H, Balaram P, Murthy MRN. Structures of Plasmodium falciparum triosephosphate isomerase complexed to substrate analogues: observation of the catalytic loop in the open conformation in the ligand-bound state. Acta Crystallogr 2002;58(12):1992–2000.

[43] Laman M, Benjamin JM, Moore BR, Salib M, Tawat S, Davis WA, et al.. Artemether-lumefantrine versus artemisinin- naphthoquine in Papua New Guinean children with uncomplicated malaria: a six months post-treatment follow-up study. Malar J 2015;14(121):1–7.